A multi-scale study of Australian fairy circles using soil excavations and drone-based image analysis

STEPHAN GETZIN [iD],[1,2],† HEZI YIZHAQ,[3] MIRIAM MUÑOZ-ROJAS,[4,5,6] KERSTIN WIEGAND,[1] AND
TODD E. ERICKSON[4,5]

[1]Department of Ecosystem Modelling, Faculty of Forest Sciences and Forest Ecology, University of Goettingen, Buesgenweg 4, 37077
Goettingen, Germany
[2]Department of Ecological Modelling, Helmholtz Centre for Environmental Research – UFZ, 04318 Leipzig, Germany
[3]Department of Solar Energy and Environmental Physics, Blaustein Institutes for Desert Research, Ben-Gurion University of the Negev,
Sede Boqer Campus 84990 Israel
[4]School of Biological Sciences, The University of Western Australia, Crawley, Western Australia 6009 Australia
[5]Kings Park Science, Department of Biodiversity, Conservation and Attractions, Kings Park, Western Australia 6005 Australia
[6]Centre for Ecosystem Science, School of Biological, Earth and Environmental Sciences, The University of New South Wales, Kensington,
New South Wales 2052 Australia

Abstract.   Fairy circles (FCs) are extremely ordered round patches of bare soil within arid grasslands of southwestern Africa and northwestern Australia. Their origin is disputed because biotic factors such as insects or abiotic factors such as edaphic and eco-hydrological feedback mechanisms have been suggested to be causal. In this research, we used a multi-scale approach to shed light on the origin of Australian FCs. At a local scale, we investigated the potential cause of FCs using analyses of soil compaction and texture within FCs, the surrounding matrix vegetation, and in nearby large bare-soil areas. We found that soil hardness and clay content were similarly higher inside the FCs and in the large bare-soil areas. When compared to the matrix soils with protective grass cover, the 2.6–2.8 times higher clay content in FCs and large bare-soil areas is likely sourced via multiple abiotic weathering processes. Intense rainfall events, particle dispersion, surface heat, evaporation, and mechanical crust building inhibit plant growth in both areas. At the landscape scale, a systematic survey of 154 soil excavations within FCs was undertaken to evaluate the presence of pavement termitaria that could inhibit plant growth. We show that in up to 100% and most of the excavations per plot, no hard pavement termitaria were present in the FCs. This fact is substantiated by the observation that small, newly forming FCs are initiated on soft sand without evidence of termite activity. At the regional scale, we investigated the spatial properties of FCs and common termite-created gaps in Western Australia, using spatially explicit statistics. We mapped three 25-ha FC plots with a drone and compared them with three aerial images of typical vegetation gaps created by harvester and spinifex termites. We demonstrate that the small diameters, the lower ordering, and the heterogeneous patterns of these common termite gaps strongly differ from the unique spatial signature of FCs. Our multi-scale approach emphasizes that FCs are not trivial termite gaps and that partial correlation with termites at some sites does not imply causation. Instead, we highlight the need to study the edaphic and eco-hydrological drivers of vegetation-pattern formation in water-limited environments.

† **E-mail:** stephan.getzin@uni-goettingen.de

INTRODUCTION

The landscape scale vegetation patterns of the so-called fairy circles (FCs) are characterized by extremely ordered grassland gaps that look like polka dots from a bird's eye view. In northwest Western Australia, the typical diameters of the circles are about 4 m, and in Namibia, the diameters increase with aridity from 4 m in the south to 6 m, and even 10 m, further to the northwest (van Rooyen et al. 2004, Getzin et al. 2015a, 2016a). Scientists from various research fields such as microbiology (Ramond et al. 2014), geochemistry (Naude et al. 2011), entomology (Tschinkel 2010, Picker et al. 2012), plant physiology (Cramer and Barger 2013, Cramer et al. 2017), spatial ecology (Getzin et al. 2015a, b), and plant toxicity (Meyer et al. 2015) have investigated these mysterious FCs. With such varying disciplines and approaches, the origin of FCs is still unclear. Often, evidence of a certain correlation between the FCs and other observations such as abiotic gas (Naude et al. 2011), ants (Picker et al. 2012), sand termites (Juergens 2013), or *Euphorbia* triterpenoids (Meyer et al. 2015) has been suggested as a causal mechanism for the vegetation gaps. However, correlation with such agents often does not exist. For example, locally, excavations have demonstrated that many Namibian FCs showed no evidence of sand termites at all, past, or present, and evidence of root damage from past termites was also absent (Tschinkel 2010, 2012, Ravi et al. 2017, Sahagian 2017).

While FCs in Namibia have been known for many years, the FCs of Australia have only recently been discovered. Getzin et al. (2016a) demonstrated that these patterns are likely to emerge via vegetation self-organization. In many examples of other known vegetation gaps, regularly spaced bare-soil patches can be attributed to a self-organization process where the patterning may emerge, for example, from an adaptation of plant morphology to aridity, and from shallow soils, by means of an extended lateral root system (Barbier et al. 2008, Deblauwe et al. 2011). In such latter African examples of vegetation self-organization, the plants act together as a population-level response to aridity stress. Positive biomass-water feedbacks lead to short-range facilitation and vegetation growth, but at the same time, to long-range competition and negative feedbacks where soil water is critically depleted and bare soil remains. Such eco-hydrological processes and plant–soil interactions are characterized by strong symmetry-breaking forces that often lead to periodic vegetation patterns with a distinct wavelength (Meron 2012, 2018). The periodic vegetation patterns in water-limited environments include a variety of pattern morphologies, ranging from gaps to bands, labyrinths, and spots or hybrid states such as rings (Couteron and Lejeune 2001, Rietkerk et al. 2002, Sheffer et al. 2007, Deblauwe et al. 2008). One of the most well-known examples is so-called Tiger bush in Africa which results from the interplay between short-range plant facilitation and long-range self-inhibitory interactions originating from plant competition for resources such as water (Lefever and Lejeune 1997).

Highly ordered, self-organized vegetation patterns are also common in arid Australia, for example, where *Acacia aneura* trees form bands along hillslopes caused by interacting processes of run-off erosion and positive feedback with vegetation growth (Mabbutt and Fanning 1987, Tongway and Ludwig 1990, Ludwig et al. 2005). In line with the formation of *Acacia* bands, it has been also argued for the Australian FCs that the impact from heavy rainfall events and resultant sealing of soil surfaces primarily induces the infiltration contrast between bare and vegetated soil, and thereby causes plant self-organization (Getzin et al. 2016a). While this previous study showed that typical crusts of termite mounds differ from the weathering-induced mechanical crusts of FCs, a survey directly relating soil compaction to soil texture, such as clay content, has not yet been undertaken for Australian FCs.

One of the main challenges in confirming the origin of FCs is that the vegetation gaps are relatively stable over decades, making it difficult to observe or measure the causal processes over time and space (Tschinkel 2012). Local experiments on individual FCs may fail to account for the landscape scale connectivity (i.e., over 100s of meters) and patterns of edaphic drivers (Tschinkel 2015b). This makes the FCs fundamentally different from other more common gap patterns in grasslands where the cause is undisputed. For example, North American harvester ants of the genus *Pogonomyrmex* are well known to form small gaps in many arid to semi-arid grasslands

of the United States (Wiernasz and Cole 1995, Crist and Wiens 1996, Schooley and Wiens 2003, Tschinkel 2015a). Small gaps in grasslands, caused by hard pavements of harvester termites, can also be found throughout large parts of arid Australia (Noble et al. 1989, Abensperg-Traun and Perry 1998). As an alternative explanation for the Australian FCs, it has been suggested that harvester termites could be responsible for their formation (Walsh et al. 2016). This suggestion was based on limited diggings in the field near the town of Newman—where only two FCs were excavated—and the conclusion that pavement termitaria, which may be level with the gap's surface, would "inhibit plant growth due to their hardness and resistance to surface water infiltration" (Walsh et al. 2016). In contrast, preliminary excavations from alternative FC locations indicated that hard pavement termitaria are unlikely to be responsible for the formation of FCs (Getzin et al. 2016b). However, to date, a systematic survey of the presence of underground termitaria in the FC area near Newman has not yet been undertaken.

One of the key features of FCs, making them ultimately so interesting, is their extraordinary spatial pattern across a range of scales and their global rareness. Unlike trivial termite- or ant-induced gap patterns in drylands, FCs are extremely uncommon. They constitute a unique grassland-gap pattern that is only known from southwestern Africa around the Namib Desert and from northwest Western Australia (Getzin et al. 2016a). For Namibia, this extraordinary pattern has been described in detail with scale-dependent spatial statistics, showing that FCs not only exhibit a regular, but an extremely regular, and homogenous pattern. For instance, it has been reported that they "exhibit an exceptionally strong order that prevails equally over the landscape" (Getzin et al. 2015b).

For a long time, termite- or ant-nest patterns in drylands have been known to show spatial regularity (Noble et al. 1989, Crist and Wiens 1996, Grohmann et al. 2010, Tarnita et al. 2017). However, when such typical termite and ant examples are thoroughly analyzed with scale-dependent spatial statistics such as the so-called pair-correlation function (PCF), it turns out that they do not exhibit the extremely regular and large-scale homogeneous pattern of FCs (cf. Getzin et al. 2015b). The lack of the strong periodicity in the spacing, particularly of such termite and ant nests in water-limited drylands, indicates that the causal mechanism behind FC-pattern formation is unrelated to termites but rather related to plant competition for scarce soil moisture (van Rooyen et al. 2004, Cramer et al. 2017). Such direct comparisons of patterns are particularly insightful if spatial distributions of a known causal agent such as termites are directly compared to patterns induced by an unknown agent.

Generally, pattern–process inference based on the precise spatial signatures is helpful to identify likely or unlikely processes in the formation of vegetation structures such as FCs (Wiegand et al. 2013). Hereby, space is used as a surrogate for unmeasured processes. A priori hypotheses about the characteristics of a particular pattern in a particular ecosystem should be as specific as possible for the ecosystem under investigation (McIntire and Fajardo 2009). In the application of pattern–process inference, the focus is on identifying and excluding unlikely processes rather than on verifying likely processes, and the most parsimonious explanation for the observed pattern should be kept as a working hypothesis (Schurr et al. 2004). This methodological approach is nowadays much more efficient and easily carried out by using remote sensing and high-resolution, drone-based image analysis because drone images provide accurate information on vegetation-gap structures over large areas (Getzin et al. 2012, 2014). A regional-scale analysis of the typical signature of termite-created gaps vs. FCs may thus help to shed light on the spatial differences and thereby on the mechanisms driving the formation of the fairy-circle patterns. For example, true ecosystem engineers such as harvester ants create regularly spaced gaps in grass vegetation over a large precipitation range of 200-600 mm annual rainfall in many ecosystems of North America (Nicolai et al. 2010, Dibner et al. 2015). In Australia, we would expect that such ecosystem engineers would cause spatial patterns that are similar to the FCs, if they were the cause.

To substantiate our preliminary knowledge on soil texture and underground termitaria in FCs and on the spatial patterning of Australian FCs vs. trivial termite-induced gaps, we applied a multi-scale approach and investigated three main hypotheses:

1. Local scale (hundreds of meters): A high clay content, and associated high soil compaction at the surface, is responsible for the inhibition of plant growth in the open FC patches, as well as in nearby large bare-soil areas that lack grass vegetation for hundreds of meters.

2. Landscape scale (thousands of meters): a) The bare soil of FCs is not caused by pavement termitaria that typically inhibit plant growth in many regions of Australia via hard termite chambers within 5 cm of the surface. b) Underground soil conditions do not principally inhibit plant growth via a hard layer.

3. Regional scale (hundreds of kilometers): Based on a regional-scale comparison in Western Australia, the characteristic spatial patterns of common gaps created by termites do not match the typical spatial properties of FCs. More specifically, harvester-termite gap patterns a) are smaller in diameter than the FCs, b) are less ordered than the spatial patterns of the FCs, and c) are typically heterogeneous at large scales.

These hypotheses were systematically investigated by employing analyses of soil compaction and soil texture, extensive field excavations, and drone technology.

Methods

Study area

From the 7th until the 25th of July 2017, we undertook fieldwork in the Pilbara region of northwest Western Australia. The fieldwork concentrated on the Australian FCs which occur within a radius of around 10–20 km east to southeast of Newman (Fig. 1, Table 1; Getzin et al. 2016a). They exist on flat terrain which is almost exclusively dominated by the grass species *Triodia basedowii* E. Pritz. This arid land receives 327 mm mean annual precipitation, and the annual evaporation is 3200–3400 mm. The annual rainfall is characterized by a strong long-term fluctuation of 37–619 mm around the mean. In the tropical cyclone season from November to April, exceptionally strong rainfall events may occur on a single day. According to the climate data of Newman Airport (Australian Government Bureau of Meteorology 2018), 40 heavy rainfall days were recorded over the last 46 yr when precipitation on rain days ranged between 50 and 214 mm (mean 78 mm per rain day). Air temperatures in the summer may be extreme with daily maxima exceeding 45°C, and soil surface temperatures on bare soil can reach 75°C inside the FCs (Getzin et al. 2016a). Soils are red, shallow, stony soils on hills and ranges, and sands on the lower lying plains comprising Red Kandosols, Red Ferrosols, and Leptic Rudosols (Isbell 2002). These soils have developed over Phanerozoic, Proterozoic, and Devonian limestone (Pepper et al. 2013).

Soil compaction and soil-texture analysis— Hypothesis 1

At the local scale, we conducted an analysis of soil compaction and soil texture in the intensively investigated plot FC-L2 and a nearby large bare-soil reference plot FC-B (see Figs. 1, 2A, Table 1). We previously showed with electron microscopy that termite crusts are different from weathering-induced mechanical FC crusts (Getzin et al. 2016a). However, to date, there is no information on potential similarity in soil compaction and soil texture of FCs and large bare-soil areas. This is of interest because similarity might potentially constitute a common cause of vegetation absence in FCs and in the typical large bare-soil areas.

For the analysis of soil compaction, measurements were taken from 16 FCs in the plot FC-L2 (Fig. 2B, C, see Hypothesis 2 below; these plots were also excavated for termite presence). Corresponding to these FC soil-compaction assessments, soil compaction was measured in grass-free spots of the matrix (*n* = 16) about 2.5 m away from each FC periphery. Adjoining the FC-L2 plot, that is dominated by FC grasslands, is the bare-soil plot FC-B. This plot is dominated by continuous bare soil interspersed with *Acacia* trees and a drainage line to the north and is situated about 700 m north of the FC-L2. The plot is characterized by exposed large bare-soil areas stretching over hundreds of meters in the surroundings (Fig. 2A). Again, 16 locations were used to measure soil compaction. These locations were randomly selected within large bare-soil areas of the exposed vegetation-free spots.

Soil compaction was measured with a pocket penetrometer prior to sampling soil texture to
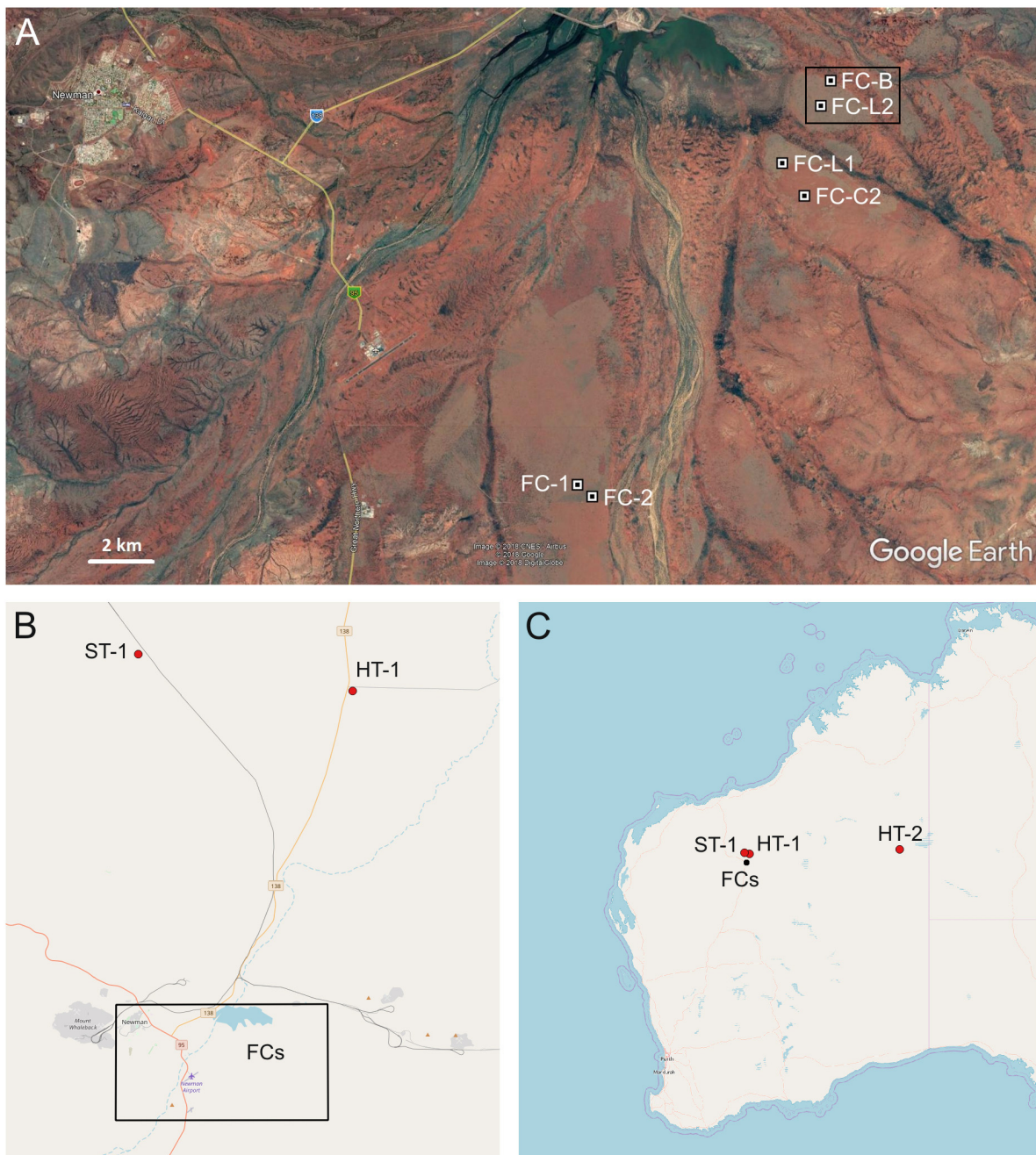
Fig. 1. Locations of the multi-scale study plots. At the local scale (A, inset), fieldwork particularly focused on our intensively investigated plot FC-L2 and also on the nearby large bare-soil plot FC-B. Soil compaction and soil texture were analyzed for the plots FC-L2 and FC-B. Fairy circles were excavated at the landscape scale east of Newman, spanning over a linear distance of around 12 km (A). Fairy-circle excavations were done for the plots FC-L2, FC-L1, FC-C2, FC-1, and FC-2. Drone images were analyzed for the plots FC-L2, FC-C2, and FC-1 (A). At the regional scale in Western Australia (B, C), the drone-mapped fairy-circle plots were contrasted to patterns of typical termite gaps and termite mounds of the Pilbara region (HT-1, HT-2, ST-1).

Table 1. Description of the different plots used in this multi-scale approach to study the Australian FCs.

Scale and type of observation	Plot name	Name in Getzin et al. (2016a)	Coordinates	Applied measurements
Local				
Soil compaction/ texture analysis	FC-L2	L2	23°21′33″ S, 119°54′52″ E	Soil compaction in 16 FCs and 16 vegetation matrix locations, soil texture at every 2nd of these 16 locations + 4 times under plants inside FCs
	FC-B	N/A	23°21′14″ S, 119°55′02″ E	Soil compaction in 16 large bare-soil locations, soil texture at every 2nd location
Landscape				
Soil excavations	FC-L2	L2	23°21′33″ S, 119°54′52″ E	16 FCs excavated for termite presence, 3 holes per FC + 10 holes under plant
	FC-L1	L1	23°22′22″ S, 119°54′17″ E	8 FCs excavated for termite presence, 3 holes per FC
	FC-C2	C2	23°22′50″ S, 119°54′37″ E	8 FCs excavated for termite presence, 3 holes per FC
	FC-1	N/A	23°26′52″ S, 119°51′11″ E	8 FCs excavated for termite presence, 3 holes per FC
	FC-2	N/A	23°27′02″ S, 119°51′24″ E	8 FCs excavated for termite presence, 3 holes per FC
Regional				
Aerial image analysis	FC-L2	L2	23°21′33″ S, 119°54′52″ E	Gap-diameter distributions and spatial patterns analyzed in 500 × 500 m
	FC-C2	C2	23°22′50″ S, 119°54′37″ E	Gap-diameter distributions and spatial patterns analyzed in 500 × 500 m
	FC-1	N/A	23°26′52″ S, 119°51′11″ E	Gap-diameter distributions and spatial patterns analyzed in 500 × 500 m
	HT-1	N/A	22°59′01″ S, 120°0′03″ E	Gap-diameter distributions and spatial patterns analyzed in 500 × 500 m
	HT-2	N/A	22°49′05″ S, 127°43′45″ E	Gap-diameter distributions and spatial patterns analyzed in 500 × 500 m
	ST-1	N/A	22°56′31″ S, 119°44′20″ E	Spatial patterns of termite mounds analyzed in 500 × 500 m

Notes: The intensively investigated plot FC-L2 was used for high-intensity data sampling. With increasing spatial scale, the sampling effort diminished. Spatial analysis of aerial images was used as information for contrasting patterns of FCs and termite-induced gaps and mounds.

avoid destruction of the soil crusts. The lowest possible reading was 0.5 kg/cm^2, the highest was 4.5 kg/cm^2. Often, however, the penetration resistance was much higher and the readings were off the scale at >4.5 kg/cm^2. In this case, off-scale values were converted to a value of 5 kg/cm^2 in order to calculate a mean value for each site. The number of measurements taken inside the FCs varied due to the differing diameters of each circle, whereby, we took a reading from the longest side of a gap every 30 cm along a straight transect line until we reached the other side of the FC. This gave us a representative mean value for the soil compaction in the entire gap. For the 16 spot locations in the corresponding matrix, or in the large bare-soil area FC-B, we took 10 individual measurements at each spot and calculated the mean.

For the assessment of soil texture, samples were taken from the top 3 cm of the soil surface from every second FC excavated for termite presence and used for soil-compaction analysis in

plot FC-L2 ($n = 8$). Soil samples from each of three diggings (Fig. 2D) were mixed and homogenized into one sample bag per FC. Additionally, when *Triodia* plants were present inside a FC, we took soil samples from the top 3 cm beneath one *Triodia* plant per gap to test whether there was a difference in texture between bare soil and soil under plants inside the gap ($n = 4$). Also, every second location in the matrix ($n = 8$) and large bare-soil area FC-B ($n = 8$), respectively, was used for the soil-texture analysis and samples were again taken from the upper 3 cm of the soil surface. Samples were air-dried and sieved to <2 mm and used for physical analysis. Soil particle size was analyzed by laser diffraction using a Mastersizer 2000 (Malvern Instruments, Malvern, UK) after removal of organic matter with H_2O_2.

Fairy-circle excavations—Hypothesis 2

At the landscape scale, we systematically excavated 154 holes in 48 FCs at five different plots in

Fig. 2. Illustration of soil analysis and soil excavations at the local scale. Soil texture and soil compaction were compared between the bare soil within FCs and the vegetated matrix samples of the fairy-circle plot FC-L2 and

(Fig. 2. *Continued*)
the large bare-soil plot FC-B, respectively. FC-B has large bare-soil areas and is located 700 m to the north of FC-L2 (A). In the plot FC-L2, soil was excavated at 16 FCs (locations indicated by arrows) (B). Example of a 4.9 m long and 4.3 m wide FC in the plot FC-L2 where 20 cm deep holes were excavated and soil samples taken (C). Example of the three diggings inside a FC (D). The same fairy circle as in (C) showing that plant growth was not hampered by any hard layer underneath the grass (E). A sand-covered, very hard pavement termitarium typical of *Drepanotermes* harvester termites with chambers within 5 cm of the surface (F). A flat but visible pavement mound with local activity of termites (G). The scale bar in (C, E) is 0.5 m long, and the ruler in (F, G) is 0.3 m long.

the area east and southeast of Newman, spanning over a linear distance of around 12 km (Fig. 1A, Table 1). In each FC of variable diameter, one hole approximately 20 cm deep and 20 cm wide was excavated in the center of the circle. Another two holes were dug in the FCs ~1–1.5 m apart along a straight line, each in opposite directions from the central hole (Fig. 2D). All diggings were done using an electric jack hammer and a pickaxe. We used this design, with three holes per FC, to assure that we accounted for variability in the underground soil properties within large parts of the gaps, and thus, we avoided a biased point sampling.

We excavated three holes in each of the FC plots FC-L2, FC-L1, FC-C2, FC-1, and FC-2 (Table 1). In the intensively investigated plot FC-L2, we investigated 16 FCs (Fig. 2B), while in the other plots, we investigated eight FCs. Additionally, for 10 FCs in FC-L2 with alive *Triodia* plants present, we dug a fourth hole directly underneath the hummock grass after cutting the plant into two halves (Fig. 2E). Thus, a total of 58 individual excavations were done in FC-L2.

In each plot, the FCs were connected along a transect (Fig. 2B). At each of the 154 holes dug, we carefully examined the walls of the excavation for hard pavement termitaria typical of *Drepanotermes* harvester termites which appear as shadowed hollows and exposed termite chambers within 5 cm of the surface (see Fig. 2F). Following this, and in the absence of termite chambers in the form of hard pavements, we recorded any evidence of termite activity. Such weaker signs of termite activity were either the sighting of termite individuals in the excavated soil dump or a gallery channel with evidence of clipped grass culms that could stretch through the FC. For each of the 48 FCs, we also recorded the number of aboveground pavement mounds

that were clearly visible at the surface of the gap (Fig. 2G). Furthermore, we counted the number of individual *Triodia* grasses that were growing inside the FCs.

Drone survey and aerial image analysis— Hypothesis 3

At a regional scale, we analyzed aerial images from FCs east and southeast of Newman and compared them to typical gap patterns created by *Drepanotermes* harvester termites and mound patterns of spinifex termites (*Nasutitermes triodiae*) outside the FC area (Figs. 1, 3). In total, we analyzed six plots consisting of three FC plots and three termite plots. Five plots closer to the Newman area were mapped with very high-resolution images taken by a drone, and a sixth plot in the Kiwirrkurra area of central Australia (i.e., HT-2; Fig. 1C) was mapped with a conventional aerial image. Feature detection was harmonized for comparability among plots and with image resolutions published in other literature (see comment in this section on used threshold value). All plot descriptions and coordinates are listed in Table 1.

For the drone surveys, we used a *Microdrone md4-1000* quadcopter (Fig. 3F). We mapped five 500 × 500 m plots using the 24-megapixel photo camera SONY NEX-7 with a wide-angle lens of 16 mm (24 mm equivalent at full-frame format). The drone flew at 90 m above ground at a speed of 4 m/s, and the plots were mapped with 80% forward and 50% sideward overlap of images. The camera was set to an aperture priority of f/5.6 and an ISO speed of 400, allowing short shutter speeds of 1/2000 under clear skies.

Three of the plots mapped represent typical *Triodia basedowii* grasslands with large FCs: FC-1, FC-C2, and FC-L2 (Fig. 1A). FC-1 was about 15 km southeast of Newman. The FC-C2 plot

Fig. 3. Impressions of FCs, gaps created by harvester termites, spinifex termite mounds, and research equipment. A spatially homogeneous and strongly ordered FC pattern of the plot FC-C2, taken with a drone at 90 m above ground (A). The median diameter of gaps in this plot was 4.3 m. Ground image of a typical large FC in the plot FC-C2 (B). A spatially heterogeneous and less ordered pattern of gaps created by harvester termites at the plot HT-1 at Jigalong Road 50 km northeast of Newman, Australia (C). The image has the same scale as (A) and was also taken 90 m above ground. Ground image of a typical small termite gap in the plot HT-1 (D). The scale bar in (B, D) is 0.5 m long. View over the large mounds (arrows) created by spinifex termites at the plot ST-1 (E). The quadcopter *Microdrone md4-1000* and its base station used in this survey (F).

burnt completely in November 2014, but after three rainy seasons, has already shown strong vegetation recovery with *Triodia* grass hummocks growing to at least 20 cm tall (Fig. 3A, B).

Plot HT-1 is located at Jigalong Road 50 km northeast of Newman and exhibits a typical gap pattern created by common Australian *Drepanotermes* harvester termites (i.e., the termite location mentioned by Walsh et al. [2016]). Our ground observations confirmed that all termite gaps in this plot had a very hard cemented pavement. The rock hard soil surface is easily recognized even by simple hammering with a wooden stick on the gap surface. The termite chambers have a characteristic hollow sound which reflect the termite-nest structure. When opened, all of these termite gaps showed within the first 5 cm termite galleries and termite chambers. The dominant grass species in HT-1 was *Triodia pungens,* and the terrain was also very flat (Fig. 3C, D). The fifth drone-mapped plot ST-1 was located 45 km north of Newman, west of the railway line. Here, within *Triodia* grassland, commonly observed larger termite mounds have been created by the spinifex termite *Nasutitermes triodiae* (Fig. 3E). The mounds may have diameters of 1–3 m and heights of up to 4 m (Abensperg-Traun and Perry 1998). This plot was mapped because the large mounds can erode over time and induce a vegetation gap.

For the sixth plot, and in order to assess an additional spatial pattern of *Drepanotermes* harvester termites, we purchased an RGB orthophoto from Landgate (https://www.landgate.wa.gov.au/), showing a 500 × 500 m plot, HT-2, at Kiwirrkurra 820 km east of Newman. According to Walsh et al. (2016; Table 1), this location is like HT-1 and is a typical example for gaps created by *Drepanotermes* harvester termites. This conventional aerial image had a resolution of 10 cm/pixel.

All the 232 drone-based images per plot were processed in OneButton software (www.icaros.us) to stitch an orthorectified and geo-referenced aerial image that covers 500 × 500 m. The final orthophotos had a resolution of 3 cm/pixel. The high resolution of the drone images allowed a precise comparison between gap patterns of the mapped plots (i.e., comparing FC, harvester termite, and spinifex termite patterns).

However, for the purpose of making our drone-based analysis comparable to other pattern analyses of coarser resolution satellite or aerial imagery (Getzin et al. 2015a, b), we used a threshold value of 2 m for the smallest gap diameters. This value also assured that a bare-soil patch was clearly defined as a typical gap and not a random opening in the matrix vegetation because smaller irregularly shaped gaps in the sparsely populated spinifex grasslands may often be an inherent property of the arrangement of individual grass hummocks during succession from a destructive fire event. Also, in the termite plot HT-2 near Kiwirrkurra, the grassland tussocks had such a low density that a minimum threshold of 2 m diameter had to be applied for safe identification of gaps.

All FC and all termite gaps within the plots were delineated to create shapefiles (a geospatial vector format digitized with QGIS-2.18 software, https://qgis.org/en/site/). Thus, for each gap, we created one shapefile with geo-referenced information on the circle's x,y-coordinate, area, perimeter, and diameter. These data allowed us to assess the diameter sizes of all gaps within a plot, the percentage bare-soil area covered by these gaps, and their scale-dependent spatial patterns. For the plot ST-1 with large termite mounds, only point locations with x,y-coordinates were digitized without information on the diameter because the tall mounds may have diameters below two meters but are still clearly identifiable due to their size-induced shadows.

Spatial pattern analysis

Scale-dependent spatial statistics, that is, the non-cumulative PCF and the cumulative Ripley's *K*-function (its *L*-transformation), were previously used to describe the typical characteristics of FC patterns (Getzin et al. 2015a, b). The PCF or *g*-function $g(r)$ is the expected density of points at a given distance *r* of the typical point, divided by the intensity λ of the pattern. This neighborhood-density function is particularly suitable to highlight critical scale effects across the landscape and the strength of ordering in a pattern (Perry et al. 2006). It is a very efficient tool to reveal whether a pattern has a strong spatial periodicity or wavelength that is typical for extremely ordered patterns. Under the null model of complete spatial randomness (CSR), the function $g(r) = 1$. Simulations of the CSR model are used to build simulation envelopes that

indicate whether deviations of the PCF from g $(r) = 1$ are significant. Thus, if $g(r)$ is for large scales r within the simulation envelopes of CSR, a pattern can be described as homogeneous (Wiegand and Moloney 2014). Values of $g(r) = 0$, specifically at short scales r, indicate that the PCF did not detect any point in the neighborhood. Otherwise, significant values of $g(r) < 1$ indicate regularity, while $g(r) > 1$ indicates aggregation (Illian et al. 2008). If the PCF strongly fluctuates at small distances around the simulation envelopes and the value of $g(r) = 1$, this indicates an extremely ordered pattern with a distinct density peak at the radius where the first six, approximately equally spaced, nearest neighbors occur. The strong periodicity of the pattern is thus indicated by $g(r) = 0$ at shortest scales (no FCs in immediate neighborhood), then a steep high amplitude of $g(r)$ far above the upper simulation envelope (six nearest-neighbor FCs detected all at same radius), followed by a steep negative amplitude (empty space behind the first six FC neighbors) which is clearly below the lower confidence envelope of the null model (Appendix S1: Fig. S1; Getzin et al. 2015b). Note that this significant fluctuation of the PCF around the null model may not necessarily be detected with small plot sizes of 200 m side length because not enough FCs could go into the analysis.

Additionally, to the non-cumulative PCF, the L-transformation (L-function) of Ripley's cumulative K-function, $L(r) = (K(r)/\pi)^{0.5} - r$, was used to accurately assess departures from CSR at larger scales between 50 m and 250 m (Wiegand and Moloney 2014). Under CSR, $L(r) = 0$ and values of $L(r) < 0$ indicate regularity, while values of $L(r) > 0$ indicate aggregation. Hence, if the L-function, after the first small-scale deviations from CSR, moves consistently into the envelopes of the simulated CSR null model, this indicates a pattern that is large-scale homogeneous. In contrast, significant departures from the CSR null model at these large scales indicate that a pattern is heterogeneously distributed at the landscape. The patterns of FCs are characterized by the combination of the characteristic fluctuation of the PCF around the null model, as described above, combined with large-scale homogeneity in the L-function (Appendix S1: Fig. S1).

The obtained spatial correlation functions $g(r)$ and $L(r)$ of the patterns were tested against CSR using the 5th-lowest and 5th-highest values of 199 Monte Carlo simulations for getting approximately 95% simulation envelopes (Wiegand and Moloney 2014). All analyses were carried out using R-software (package spatstat, http://www.R-project.org/).

RESULTS

Soil compaction and soil-texture analysis— Hypothesis 1

In regard to the soil compaction and texture analyses, there were three striking results. Firstly, the highest clay contents were found inside the FCs in plot FC-L2 (4.9%) and even higher in the large bare-soil area of plot FC-B (5.4%; Table 2). Compared with the soil within the matrix vegetation, the clay contents inside the FCs and in the large bare-soil areas were 2.6 and 2.8 times larger, respectively. Secondly, compared with the soil within the matrix vegetation, the soil-compaction values inside the FCs and in the large bare-soil areas were 2.6 and 2.1 times higher, respectively.

Table 2. Summary of the soil texture within the top 3 cm of the soil profile and soil-compaction analysis.

Soil	Inside FC	Inside FC under plant	Matrix	Large bare-soil area
Clay, % (SD), <0.002 mm	4.9 (0.6)*	2.0 (1.0)	1.9 (0.6)	5.4 (0.8)*
Silt, % (SD), 0.05–0.002 mm	13.3 (2.3)*	6.2 (2.6)	4.9 (1.1)	12.3 (1.2)*
Sand, % (SD), 2–0.05 mm	81.8 (2.8)*	91.8 (3.5)	93.3 (1.6)	82.4 (1.5)*
Compaction, kg/cm^2 (SD)	4.6 (0.3)*	Not measured	1.8 (0.5)	3.7 (0.5)*

Notes: Shown are mean values (and standard deviations). Absolute percentage values of clay, silt, and sand differ in comparison with the data published in Getzin et al. (2016a) because particle size distribution was obtained from a ANALYSETTE laser diffractometer for that study, versus from a Mastersizer analyzer in this study. Nonetheless, the relative percentage values are similar: Clay contents were about 2.6 times higher in the gap centers as compared to the matrix soil. One-tailed t-tests were performed to compare the soil texture and compaction values of the soils of the matrix with the inside of FCs and large bare-soil areas, respectively. t-tests were also performed to compare the means of the large bare-soil areas directly with the inside of FCs. All tests revealed non-significant differences between these latter two groups.

 * Indicates highly significant differences between the means of the samples at $P < 0.001$.
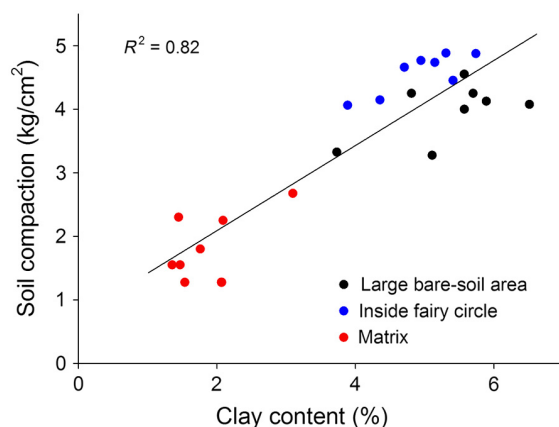
Fig. 4. Soil compaction which inhibits vegetation inside the FCs of plot FC-L2 and similarly in the large bare-soil areas of plot FC-B (see also Fig. 2A) was directly dependent on clay content in the upper soil layer. Mean clay content in the large bare-soil area was 5.4%, even higher than the 4.9% inside the FCs, albeit the difference was not significant. In contrast, clay content and soil compaction were significantly lower in the soils of the matrix vegetation in plot FC-L2.

These differences in direct comparison to the soils of the matrix vegetation were all highly significant. In contrast, the soil texture and soil-compaction values between FCs and the large bare-soil areas were not significantly different, indicating that their cause is very similar. As expected from these results, high clay contents correspond directly with the measured soil compaction, leading to a strong correlation with an R^2 value of 0.82 (Fig. 4). Lastly, under alive *Triodia* plants growing inside the FCs, the clay content was 2.0%, effectively as low as the 1.9% in soil within the plant-rich matrix vegetation. Thus, under protective plant cover, the clay content was 2.5 or 2.7 times lower than in exposed bare soil inside the FCs or in the large bare-soil area FC-B, respectively.

Fairy-circle excavations—Hypothesis 2

In contrast to the description of Walsh et al. (2016), the 154 excavations in the FC area near Newman revealed that 139 holes (90.3%) had no pavement termitaria that could prevent plant growth or establishment via a very hard layer. Remarkably, in our intensively investigated plot FC-L2, all of the 58 holes (100%) had no pavement termitaria (Table 3). This included 10 excavated *Triodia* plants in FC-L2 that showed no sign of termite activity below the plant, which would have been evidenced as either pavement termitaria, single galleries, or termite individuals. Only one of the 16 FCs in FC-L2 had two flat aboveground termite mounds at the gap periphery, and these mounds had small diameters of only 50 cm. Moreover, in the plot FC-L2, numerous young FCs can be found which have small diameters of only 2–2.5 m. These immature gaps develop to circular arrangements of plants on soft sand without any evidence of termite activity (Fig. 5).

Also, in FC-L1 and FC-C2, 92% of all holes had no underground pavement termitaria. Only the nearby plots FC-1 and FC-2 showed a somewhat higher presence of underground termitaria and aboveground mounds. But even here, 87% and 67% of all excavated FCs, respectively, had no pavement termitaria. Overall, the percentage of excavations with weak signs of termite activity such as the occurrence of a single gallery, with or without termites, was very low and variable in all five excavation plots.

All investigated plots had a high percentage of FCs where plant growth was not fully restricted. Most FCs did show signs of plant growth with up to 11 individual *Triodia* plants growing inside the gap (Table 3). These FCs with alive *Triodia* plants growing either in the center or toward the edges of the gaps indicate that plant growth was principally not restricted by a long-lasting

Table 3. Summary of the main findings of fairy-circle (FC) excavations.

| Parameter	FC-L2	FC-L1	FC-C2	FC-1	FC-2
Number of excavated FCs in study plot	16	8	8	8	8
Number of individual excavations in study plot	58	24	24	24	24
Percent holes with underground pavement termitaria	0	8	8	13	33
Percent holes with a gallery or termite individuals	10	21	4	29	13
Number of FCs with aboveground termite mounds	1	1	1	7	7
Number of FCs with living *Triodia* plants in gap	11	6	5	1	7
Maximum number of living *Triodia* plants in gap	11	5	5	6	1
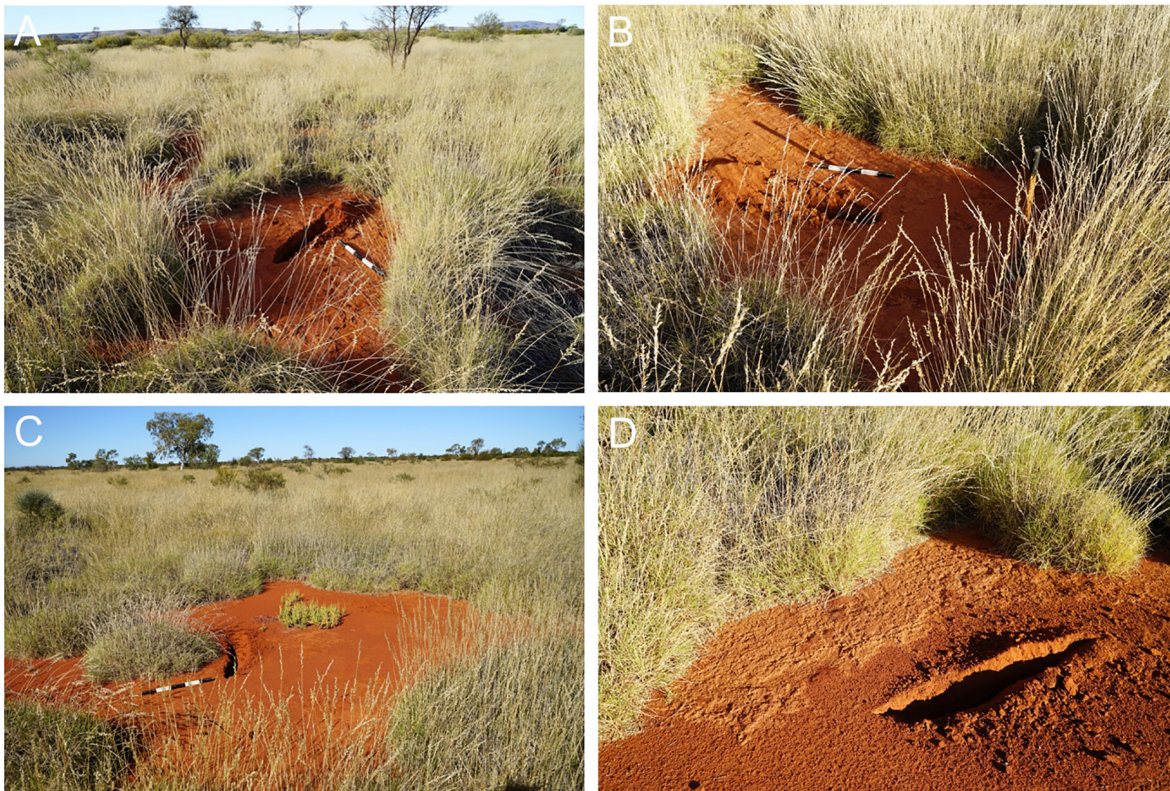
Fig. 5. Close-up images of young FCs. Small, immature gaps develop in the plot FC-L2 within the grassland matrix (A–C). Their size of around 2-2.5 m is similar to those mature gaps created by harvester termites at the Jigalong Road site (HT-1 plot), but the substrate is soft sand and termite signs are fully absent. These gaps are already characterized by a wall of fused *Triodia* plants that prevent the outflow of rainfall water. As a consequence, mechanical crusts develop at the gap periphery where water cannot escape (B, D). The scale bar in (A–C) is 0.5 m long.

cemented underground layer such as pavement termitaria (see also Appendix S1: Fig. S2).

Drone survey and aerial image analysis—Hypothesis 3

The diameter distributions differed strongly between FCs and gaps created by harvester termites. The modes for the FC diameters of FC-1, FC-C2, and FC-L2 were 4.6 m, 4.2 m, and 4.4 m, respectively. In contrast, size distributions of termite gaps HT-1 and HT-2 were strongly skewed toward small diameters to the left and the modes —the most common diameter values—were only 2.5 m and 2.2 m, respectively (Fig. 6). Thus, most FCs were about 2 m larger in diameter than the termite gaps. This is also indicated by the comparison of the median of diameters and the range. Median diameters of FCs in the plots FC-1, FC-C2, and FC-L2 were 4.3 m, 4.3 m, and 3.7 m, respectively. Fairy circles in FC-1, FC-C2, and FC-L2 reached large sizes, ranging 2.0–7.1 m, 2.0–6.4 m, and 2.0–6.2 m, respectively. Median diameters of termite gaps in HT-1 and HT-2 were 2.7 m and 2.4 m, respectively. These gaps in HT-1 and HT-2 ranged in diameter 2.0–4.3 m and 2.0–3.9 m, respectively. Hence, the median value of FCs corresponds to the largest termite gaps found within plots HT-1 and HT-2.

In addition, the total area of bare circular patches that covered the 25-ha plots differed strongly between FCs and termite gaps. In the FC plots, FC-1, FC-C2, and FC-L2 gaps covered 10.2%, 10.4%, and 8.1% of the surface, respectively. In contrast, the small termite gaps in HT-1 and HT-2 covered only 1.5% and 1.2% of the area, respectively.
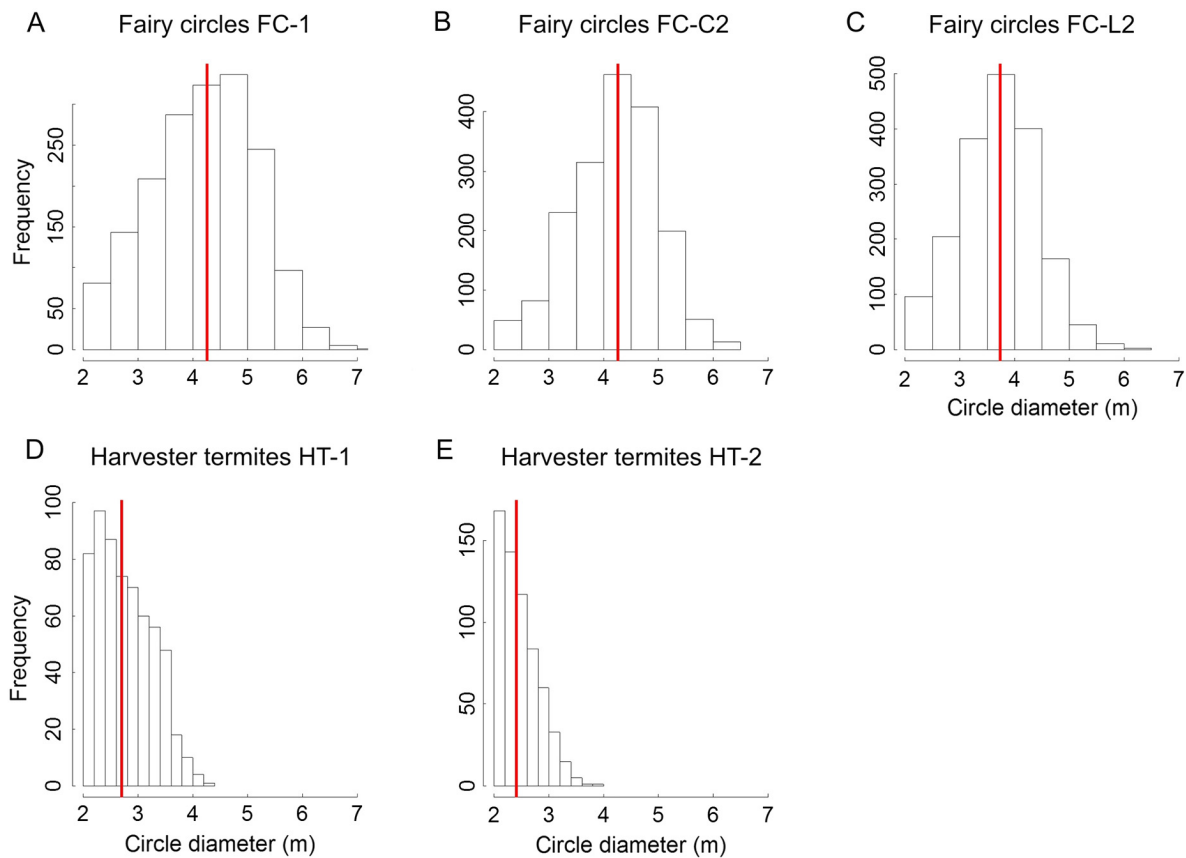
Fig. 6. Histograms of the diameter distributions of FCs (A–C) and gaps created by harvester termites (D, E). The red vertical lines show the median diameter because the data of harvester-termite gaps (D, E) are highly skewed. No data are shown for the plot ST-1 because only the point location of the tall termite mounds was measured (see *Methods*).

Spatial pattern analysis

Within the six 25-ha plots FC-1, FC-C2, FC-L2, HT-1, HT-2, and ST-1, we digitized a total of 1754, 1809, 1803, 607, 627, and 116 gaps, respectively. The mean nearest-neighbor distances (and their coefficient of variation) in the FC plots FC-1, FC-C2, and FC-L2 were 9.9 m (0.15), 9.8 m (0.15), and 9.6 m (0.15), respectively. In contrast, in the termite plots HT-1, HT-2, and ST-1, these values were much larger with 13.4 m (0.32), 11.5 m (0.37), and 21.1 m (0.72), respectively.

All FCs showed the typical four spatial characteristics that jointly define them: (1) at smallest neighborhood scales up to circa $r = 3$ m, $g(r) = 0$ which indicates the empty space between the focal circle and the first nearest neighbors, with increasing distance r, (2) there is

a strong amplitude with a high positive peak of $g(r)$ above the null model (six nearest-neighbor FCs detected all at same radius), followed (3) by a strong second significant negative peak below the lower simulation envelope (empty space behind the first six FC neighbors), and (4) at large scales the L-function stays within the simulation envelopes of the homogeneous Poisson null model (CSR), meaning that there is no significant variation in FC density across the plot. All three FC examples showed this identical periodicity and extreme ordering of the pattern (Fig. 7).

In comparison, all three termite examples showed patterns clearly different from the FC patterns. Neither the HT-1 nor the HT-2 pattern showed zero values of $g(r)$ for smallest
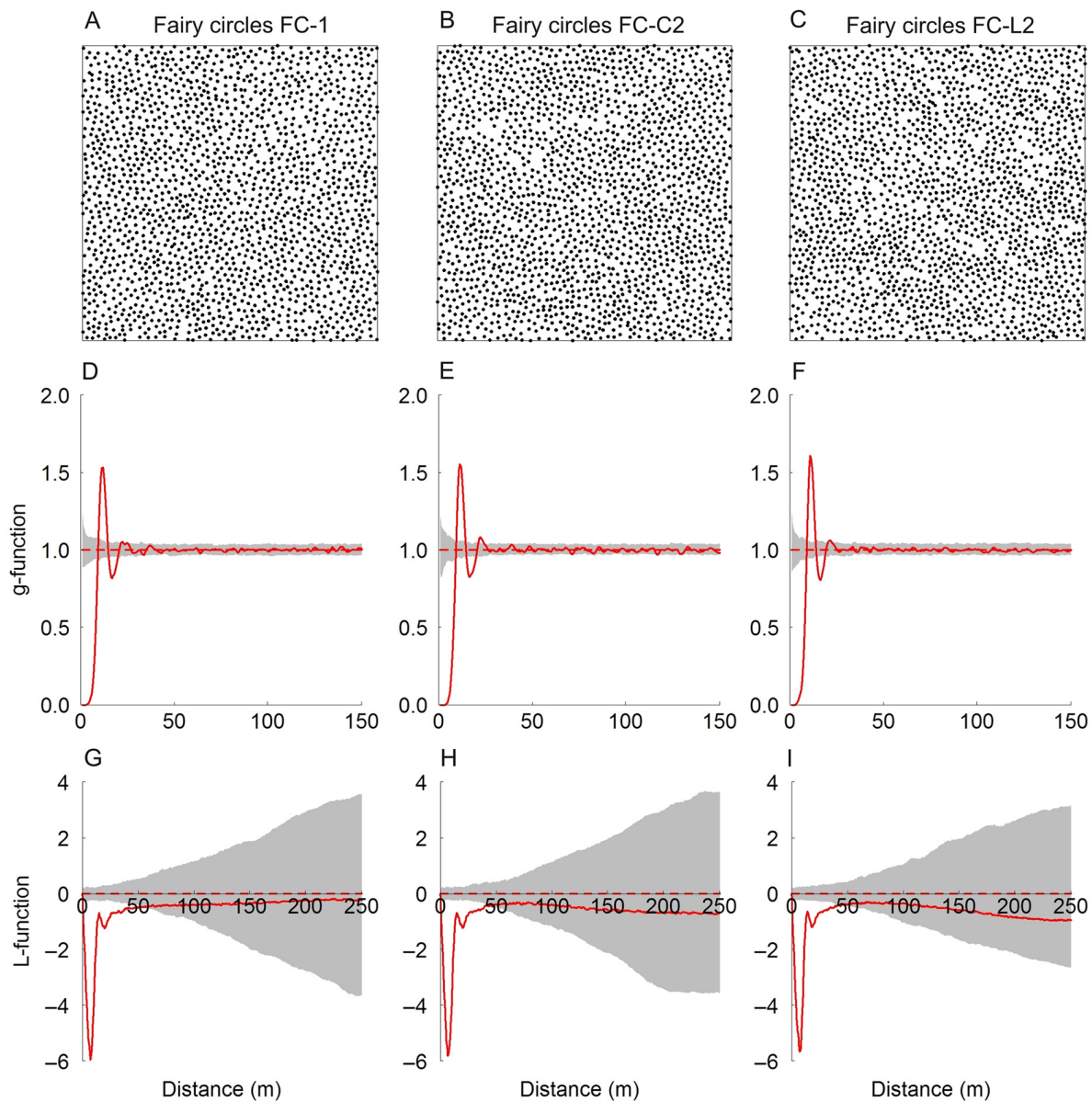
Fig. 7. The spatial distribution patterns of FCs are shown for the three 500 × 500 m drone-mapped plots (A–C). The patterns were contrasted to random null models, using the pair-correlation function $g(r)$ (D–F) and the L-function (G–I). The y-axes in (D–F) were scaled to a maximum radius of 150 m distance to better emphasize the small-scale behavior of the g-function. The pattern is regular and aggregated at circular neighborhood distances r if the red line of $g(r)$ or $L(r)$ is below the lower and above the upper gray simulation envelopes, respectively. Approximately 95% simulation envelopes were constructed using the 5th-lowest and 5th-highest value of 199 Monte Carlo simulations of the CSR null model.

neighborhood distances where the red line of the PCF would touch the *x*-axis, meaning that the PCF did detect termite gaps at these smallest distances (Fig. 8D, E). The ST-1 termite mounds were even significantly and strongly aggregated up to small scales of $r = 12$ m (Fig. 8F). Also, none of the termite examples showed the fluctuation of the PCF around the upper and lower null
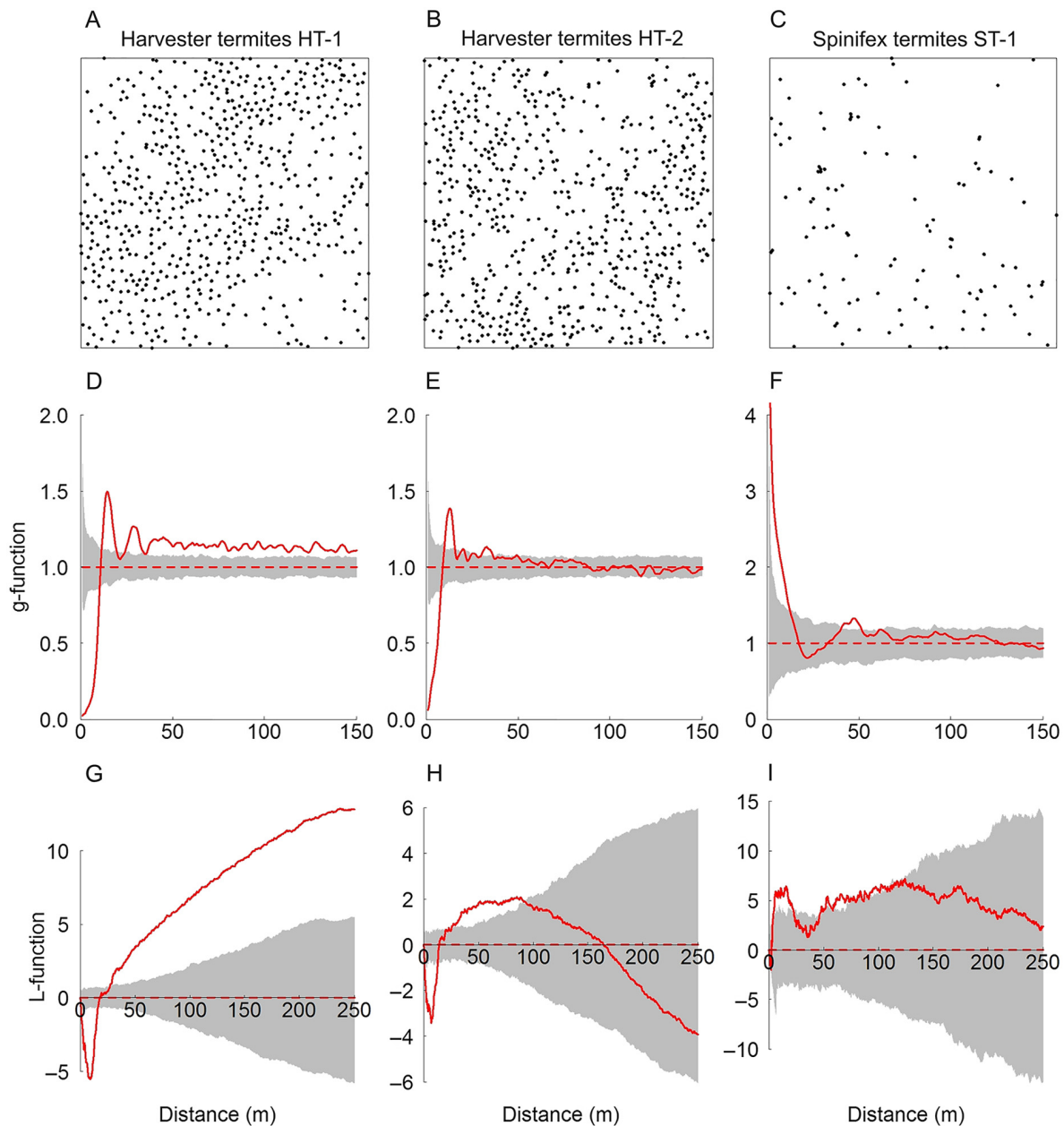
Fig. 8. The spatial distribution patterns of gaps created by harvester termites (A, B) and of large termite mounds created by spinifex termites (C), shown for the 500 × 500 m plots. The patterns were contrasted to random null models, using the pair-correlation function $g(r)$ (D–F) and the L-function (G–I). For details, see Fig. 7. The pattern is heterogeneously distributed and clusters at the landscape scale if the red line of $L(r)$ is at larger distances >50 m above the upper gray simulation envelopes of the homogeneous Poison null model, CSR.

model envelopes. Most strikingly, all termite examples did show heterogeneous distributions at large scales, as indicated by the L-function which, after the first small-scale deviation from CSR, did not move into the simulation envelopes thereafter between 50 and 100 m radius (Fig. 8G–I). The most heterogeneous pattern with strong variations in local gap densities

across the plot is demonstrated by the harvester termite HT-1 at Jigalong Road (Fig. 8G).

DISCUSSION

The Australian FCs tally with the Namibian FCs in all unique pattern signatures, making them an ideal reference ecosystem for drawing analogies about universal principles of vegetation-pattern formation in drylands (Meron 2018). In this study, we aimed to investigate in greater detail the origin of the Australian FCs based on a multi-scale study moving from a detailed local survey, via a landscape scale assessment, to regional scale observations. In the following, we will discuss the three investigated hypotheses starting at the local scale.

Soil compaction and soil-texture analysis— Hypothesis 1

One landscape characteristic of Australia's vast outback is the presence of large bare-soil areas that are lacking continuous grass vegetation cover over hundreds or thousands of meters. The fact that in our study the highest clay contents at the surface were found in the large bare-soil areas and in the interior of FCs, and termite mounds were largely absent in our study area (cf. Table 3), particularly FC-L2, indicates that the origin of the plant-inhibiting clay crusts is independent of termite mounds. Using SEM-EDS-chemical analysis of elemental mass fraction and electron microscopy, we previously showed that termite-induced crusts differ from mechanical crusts in terms of elemental composition. Also, mechanical crusts were much thinner, less hard, and the gap centers had both, significantly higher amounts of clay and significantly lower infiltration rates than the vegetation matrix (Getzin et al. 2016a, b). Here, we found, in large bare-soil areas and FCs, both the high clay content at the soil surface and the associated high soil compaction ($R^2 = 0.82$, Fig. 4) likely reduced the presence of established perennial plants, just as it is known from many other vegetation-deficient run-off sources in Australia (Saco et al. 2007, Dunkerley 2010). Clay contents were even higher in the large bare-soil area than inside the FCs, but the non-significant difference indicates that the cause of these high clay contents is very similar. The existence of large bare-soil patches next to vegetated areas with FCs, resulting from a high ratio of evaporation rate to infiltration rate, has been also directly predicted by a process-based model (Getzin et al. 2016a, their Fig. 4). The mechanism of clay-crust formation is abiotically induced because where plants are providing crown cover, such as in the matrix or partly inside the FCs, the clay content was up to 2.8 times lower. However, in unprotected soil without vegetation, particle dispersion after heavy rainfall leads to the filling of air spaces in the soil with fine particles of clay, which seals the substrate.

Fairy-circle formation in a wider context of plant self-organization

Self-organized vegetation patterns in arid Australia are relatively stable and may evolve over hundreds of years (Saco et al. 2007). They are functionally related to hydrologic processes by determining soil moisture patterns, run-off redistribution, and evapotranspiration. Such run-off–run-on systems may operate at small scales of a single plant, but also at larger scales, leading to periodic grassland or mulga patterns in many Australian drylands (Dunkerley 2010). The vegetation-deficient run-off sources have commonly a low porosity, sealed surfaces and experience strong mechanical impact from raindrops. Splash erosion and raindrops that cause particle dispersion and mechanical crusts at the exposed topsoil layer likely have a great impact in the FC area near Newman. This is because heavy rainfall events of more than 70 mm per day occur at recurrent intervals during cyclone events in summer and soil surface temperatures of up to 75°C and high evaporation rates alter the unprotected soil surfaces, leading to the typical physical crusts that can be seen in the gaps (Fig. 5B, D; Getzin et al. 2016a, b). Australian soils are known for their continuing emergence of carbonate horizons, strongly weathered red earths (kandosols), and especially in the western Australian deserts, hardpan formation is common at shallow layers of only 0.3–1.0 m depth (Morton et al. 2011). It is also well known from Australian plant patterns that rare events of very intensive rainfall on to unprotected bare soil play a key role for the emergence and reinforcement of vegetation patterns and spatial formation of siliceous hardpans (Mabbutt and Fanning 1987, Tongway and

Ludwig 1990, Ludwig et al. 2005). Thereby, feedbacks from plant growth maintain nutrient levels and protect the soil from rainfall-induced erosion. In this respect, it is remarkable that *Triodia* grasses demonstrate a high phenotypic plasticity by growing as gap-like structures but also as labyrinthine and partly banded patterns (Appendix S1: Fig. S3), a pattern transition that is facilitated by surface run-off but does not evolve on deep aeolian sands in Namibia (Goudie and Viles 2015). It is likely that the extreme rainfall and temperature fluctuations at the iron-rich and acidic soils near Newman cause over hundreds of years intense cycles of rainwater percolation, evaporation, and precipitation of salts to form a layering of soil which is unfavorable for plant growth, particularly in the upper few centimeters where clay crusts and extreme surface heat prevent plant establishment.

Fairy-circle excavations—Hypothesis 2

Preliminary soil excavations around healthy *Triodia* plants have already indicated that pavement termitaria are not causing the FCs (Getzin et al. 2016*a*, *b*), although a systematic survey had not yet been undertaken. Pavement termitaria, where hard termite chambers occur typically within 5 cm of the surface (Fig. 2F, G), have been shown to be the primary cause of termite gaps in many parts of arid Australia (Watson et al. 1973, Holt and Easey 1985, Spain et al. 1986, Noble et al. 1989, Walsh et al. 2016), and they do partially occur within the FC area near Newman. However, our systematic survey based on 154 excavations supports our second hypothesis that plant-inhibiting pavements or abandoned ghosts of termitaria are not responsible for the bare soil of FCs.

Our results demonstrate that about 90% ($n = 139$) of all excavated holes did not show pavement termitaria, where a cemented layer could inhibit plant growth. With this, the effect of pavement termitaria was very low and spatially variable. In our intensively investigated plot FC-L2, for instance, 100% of all 58 excavations did not show any underground termitaria. Only 8% of all excavations carried out in two plots further south showed the presence of termites (i.e., chambers), and the two most southern plots toward the Newman Airport had underground termitaria in 13% and 33% of all holes

excavated. The occurrence of a single termite gallery or individual in the excavations was very low and had no systematic relationship to the occurrence of pavement termitaria (Table 3). While termites are generally abundant in these environments, the latter indicates that small individual foraging tunnels are merely a random event throughout the entire area.

The independence of FC formation from termite activity is further supported by the fact that we observed many new gaps in all investigated areas where small FCs start to form in the matrix (Fig. 5). These small, immature FCs, around 2–2.5 m in diameter, were of the same size as typical mature harvester-termite gaps, but in contrast, the sand substrate in the immature gaps was still very soft. At the densely vegetated edges where water is trapped after heavy rainfall events, the typical mechanical soil crusts form which are also dominating the mature FCs in the area. This demonstrates that already such smaller gaps appear to be of benefit to the peripheral plants because the gaps function as an extra source of water for the surrounding grass matrix. Overall, these newly appearing grassland gaps are initiated without termite activity and thereby demonstrate that the formation of a vegetation-less grassland gap does principally not require a destructive, plant-inhibiting mechanism induced by termites.

One of the most important observations during this survey was that the majority of these large FCs did have variable numbers of individual *Triodia* plants growing inside the gaps. For example, in the FC-2 plot, 88% of FCs showed some level of plant growth, and up to 11 *Triodia* hummocks have been recorded within a single FC (Appendix S1: Fig. S2, S3A). This exemplifies that the presence or absence of vegetation inside the FCs is principally not governed by a simple mechanism in the form of hard pavement termitaria. Furthermore, if aboveground termite mounds were present, their negative impact on plant growth in the large FCs was spatially very restricted. For example, Fig. 2G shows that grass establishment was not inhibited by the very close pavement cap and Appendix S1: Fig. S2A, B demonstrates that even larger *Triodia* hummocks can grow without being affected if a termite mound is situated just one meter apart. Also, it has been previously demonstrated that the number of aboveground termite signs in the FCs did

not correlate with gap size and that the spatial patterns of such clearly visible ground-mapped termite or ant signs did not correlate with the spatial FC patterns (Getzin et al. 2016*a*). If above-ground termite mounds would cause the Australian FCs via mound-induced surface crusts, it would be expected that more mounds would lead to larger gap sizes, which is not the case. These above findings underline that partial correlation with aboveground or underground termite (or ant) signs does not imply causation and that such mere correlation needs to be carefully interpreted.

Drone survey and spatial pattern analysis— Hypothesis 3

Fairy circles are not just ordinary grassland gaps which are indeed common in large parts of Australia, North America, and elsewhere. Fairy circles differ from these trivial insect-created gaps by having an exceptionally distinct and rare spatial pattern and by not having a clear causal agent, making them a long-standing, mysterious landscape scale phenomenon (van Rooyen et al. 2004, Tschinkel 2012, Sahagian 2017). The rare Namibian and Australian FCs were precisely described with scale-dependent spatial statistics (Getzin et al. 2015*b*, 2016*a*), showing that these grassland-gap patterns are unambiguously defined by two fundamental spatial properties: an extraordinary degree of spatial ordering (extreme regularity) at small scales $r < 50$ m and homogeneity at large scales. Such grassland-gap patterns are not known from any other place in the world. This identical spatial signature of the pattern qualifies the Australian FCs to be genuine FCs, just as their Namibian counterparts.

Our new drone-based data support these general findings. In accordance with our third hypothesis, there are clear differences between the common termite-created pavement gaps and the rare FCs because they significantly differ in terms of spatial patterns but also with regard to the diameters and size distributions. Harvester termites typically create small grassland gaps with diameters of only one to three meters (Watson et al. 1973, Noble et al. 1989, Abensperg-Traun and Perry 1998). Indeed, the most common diameter values of termite gaps were about 2.4 m. In contrast, the most common diameter values for the FCs were about 4.4 m (Fig. 6). Besides these

size differences, FC size distributions showed a more bell-shaped curve with largest diameters reaching 6–7 m, while the size distributions of termite gaps were skewed toward very small diameters.

Also, the spatial patterns of termite gaps and FCs are not matching. In this study, we used large observation windows of a size of 500×500 m that are suited to reveal the two fundamental properties for the FC patterns: The PCF strongly fluctuates with high amplitude positive and negative peaks around the simulation envelopes of the null model at small scales, but at large scales, the PCF and the *L*-function stay inside the null model and thereby indicate a large-scale homogeneous distribution (Fig. 7). Both pattern characteristics of these analyses are contradicted by all three Australian termite examples. The harvester termites are less ordered at small scales, and they are large-scale heterogeneously distributed with significant spatial variability in local density within the plot (Fig. 8G, H). This is also true for the termite pattern at Newhaven in the Northern Territory of Australia (not analyzed here), mentioned by Walsh et al. (2016). At this location, the clearly visible termite gaps (based on Google Earth imagery) show the same kind of heterogeneity across a few hundred meters and beyond. This variation in density is typical for harvester termites (Noble et al. 1989) and occurs, for example, at our ground-visited harvester-termite plot HT-1 (located at Jigalong Road) despite the fact that this plot was as flat and topographically homogenous as our FC plots. Due to sufficiently dense grass cover of this HT-1 plot, it was possible to also segment termite gaps down to a threshold of 1 m diameter which led to smaller median diameters of only 2.3 m. But even then, all termite gaps were heterogeneously distributed, and thus, this significant difference to FC patterns is not dependent on the 2-m resolution (*L*-function analysis in Appendix S1: Fig. S4).

The high spatial variability in termite-nest ordering is also shown by the coefficient of variation of the nearest-neighbor distances which was more than twice as high for the gaps created by harvester termites (0.32, 0.37) as compared to the FCs (0.15, 0.15, 0.15).

There are many known reasons why termite gaps commonly show a higher spatial variability

than FCs. For example, young offspring colonies often cluster around established colonies (Grohmann et al. 2010), which is demonstrated for the highly aggregated mound pattern of spinifex termites (Fig. 8C, F). Also, intraspecific competition between colonies does often not lead to differential survival and thus changes toward more regular patterns (McGlynn 2012). The number of dispersing queens may vary spatially across the landscape, or variability in colony spacing within a plot is due to variability in colony age and size (Holt and Easey 1985, Crist and Wiens 1996). In the case of harvester termites, another factor is likely responsible for the less ordered patterns. *Drepanotermes* harvester termites—like many other widespread termite species in Australia— may have polycalic nests. Using radioactive labeling, Holt and Easey (1985) demonstrated that *Drepanotermes* mounds, separated by distances of 4–10 m, belonged to the same colony. Hence, many neighboring mounds may belong to one and the same colony, making hostile interactions between members of the same genetic colony unlikely. Holt and Easey (1985) therefore emphasized that even regularity of the mounds cannot be interpreted as indicating intraspecific competition. Inconsistent spacing patterns have been also reported from a variety of termite species in Queensland, Australia (Spain et al. 1986). The less ordered and large-scale heterogeneous termite gaps in the Pilbara and in central Australia demonstrate that the ordering forces of these harvester termites have little in common with the consistently homogeneous spatial organization of FCs across the landscape. In contrast, the positions of the FCs are much more fixed in space because they are embedded in a tightly spaced grid-like hexagonal arrangement of large neighboring FCs. These spatial constraints are also exemplified by the surface coverage of 10% of FCs vs. only up to 1.5% of the termite gaps, with the latter allowing for more distance variability in the spacing.

The large size and the strict nearest-neighbor spacing homogeneously across the landscape are indicative for highly symmetrical competitive forces that take equally place over small and large scales. In the view of vegetation self-organization, the symmetrical pattern of such large grassland gaps is an expression of plant competition for soil water, where there is not enough water to sustain a uniform vegetation cover (Meron 2012, Getzin et al. 2015a, b, 2016a, Zelnik et al. 2015, Cramer et al. 2017). In contrast, based on the spatial patterns and size distributions as seen in aerial images, and particularly based on the lack of pavement termitaria in most FCs, we identify termites in this eco-region as an insubstantial candidate mechanism to cause the FCs, making plant self-organization the most likely explanation for the observed pattern (Schurr et al. 2004, McIntire and Fajardo 2009).

A dynamic perspective on vegetation patterns

Why are these FCs globally so rare? We propose that at least four particular ingredients need to spatially coincide (1) the soil substrate must be homogeneous, (2) the grassland must be mono-specifically dominated (as is the case with *Triodia basedowii* in Australia or *Stipagrostis* sp. in Namibia) or not comprise more than two species, (3) the specific plant architecture must fit the specific biomass-water feedback mechanism at the local area (e.g., strong spatial plasticity in seed-regenerating *Triodia basedowii* to react as a population-level response to water-stress on clay crusts or vertically confined *Stipagrostis* roots and soil-water diffusion in Namibian sand), and (4) the climatic stress comprising of mean annual rainfall and evaporation rate for specific edaphic conditions must allow enough plant growth to enable the formation of matrix vegetation and gaps but not too much plant growth which would lead to the permanent disappearance of gaps.

The co-occurrence of fully evolved gap patterns and still labyrinthine transitions in-between gaps such as on the flat plot FC-L2 indicates that the plants are dynamically forming the FCs (Appendix S1: Fig. S3). While there is global stability of the identical FC patterns throughout the area due to the wavelength of water competition (Deblauwe et al. 2008, Meron 2012, 2018), these patterns are probably, just like the patterns found in Namibia (Zelnik et al. 2015), subject to local modulation by rainfall fluctuations as the small emerging gaps, as well as the vegetation recovery or plant death inside the gaps shows (Appendix S1: Figs. S2, S3A). The different degrees of vegetation recovery go along with our observation that soils of the upper 20 cm had different degrees of hardness. Recurrent fire

certainly plays a key role in the dynamic recovery of this gap pattern within Australian perennial grasses while in Namibia, the local recovery with annuals is dominated by stochastic long-term rainfall fluctuation (Zelnik et al. 2015). Fire-vegetation-soil feedbacks in Australian *Triodia* grasslands are relatively stable in the long-term, and self-organized arrangements of plants, such as bands and spots in response to optimize water capture, are particularly drought resistant (Bowman et al. 2008). Australian grasses are even known to form oblique banded vegetation patterns on slopes where the grove borders are roughly orthogonal to the contour (Dunkerley and Brown 2002). It is therefore not surprising to observe a variety of labyrinthine vegetation patterns on flat terrain around the FCs (Appendix S1: Fig. S3B, C). *Triodia basedowii*, which solely recovers from seeds after fire (Rice and Westoby 2009), seems to be a highly plastic species which germinates preferentially at those locations where its growth is facilitated by having better access to run-off water (Brooker et al. 2007). These are the locations around new or mature gaps which function as an extra source of water for the plants.

Conclusions

All our field mappings of termite signs in the FC area near Newman demonstrate that there is no systematic relationship or correlation between termites and the FCs—just as it has been witnessed for Namibian FCs, too (Tschinkel 2010, 2012, Ravi et al. 2017). When looking 12 km across the landscape scale, we observed identical FC patterns, no matter whether there were 0%, 8%, 13%, or 33% pavement termitaria in a specific area. This spatial consistency of the emergent vegetation pattern indicates that the extremely ordered FCs evolve independent of local termite effects but are rather driven by the same water limitation across the landscape (van Rooyen et al. 2004). This water limitation is likely abiotically induced by weathering of the soil surface which causes also in the large bare-soil areas an absence of grass coverage. While termites and their mounds in the area are certainly locally abundant, as in nearly every spinifex grassland in Australia or savanna-desert transition in Africa, in context with the consistent formation of FCs, we have to consider them merely as spatial noise.

We conclude that partial distribution overlaps do not imply causation by the fauna that settle at these bare-soil patches or even partly alter them. Above all, zero correlation with FCs and 100% absence of termite pavements as in our intensively investigated plot is inconsistent with the idea that subterranean termitaria would cause these unique fairy-circle patterns. We suggest that the symmetry-breaking forces that globally induce the same emergent FC patterns are related to biomass-water feedbacks and plant competition for soil moisture in such arid environments.

Literature Cited

Abensperg-Traun, M., and D. H. Perry. 1998. Distribution and characteristics of mound-building termites (Isoptera) in Western Australia. Journal of the Royal Society of Western Australia 81:191–200.

Australian Government Bureau of Meteorology. 2018. Climate statistics for Australian locations. http://www.bom.gov.au/climate/averages/tables/cw_0071 76.shtml

Barbier, N., P. Couteron, R. Lefever, V. Deblauwe, and O. Lejeune. 2008. Spatial decoupling of facilitation

and competition at the origin of gapped vegetation patterns. Ecology 89:1521–1531.

Bowman, D. M. J. S., G. S. Boggs, and L. D. Prior. 2008. Fire maintains an *Acacia aneura* shrubland—*Triodia* grassland mosaic in central Australia. Journal of Arid Environments 72:34–47.

Brooker, R., et al. 2007. Facilitation in plant communities: the past, the present, and the future. Journal of Ecology 96:18–34.

Couteron, P., and O. Lejeune. 2001. Periodic spotted patterns in semi-arid vegetation explained by a propagation-inhibition model. Journal of Ecology 89:616–628.

Cramer, M. D., and N. N. Barger. 2013. Are Namibian "fairy circles" the consequence of self-organizing spatial vegetation patterning? PLoS ONE 8: e70876.

Cramer, M. D., N. N. Barger, and W. R. Tschinkel. 2017. Edaphic properties enable facilitative and competitive interactions resulting in fairy circle formation. Ecography 40:1210–1220.

Crist, T. O., and J. A. Wiens. 1996. The distribution of ant colonies in a semiarid landscape: implications for community and ecosystem processes. Oikos 76:301–311.

Deblauwe, V., N. Barbier, P. Couteron, O. Lejeune, and J. Bogaert. 2008. The global biogeography of semiarid periodic vegetation patterns. Global Ecology and Biogeography 17:715–723.

Deblauwe, V., P. Couteron, O. Lejeune, J. Bogaert, and N. Barbier. 2011. Environmental modulation of self-organized periodic vegetation patterns in Sudan. Ecography 34:990–1001.

Dibner, R. R., D. F. Doak, and E. M. Lombardi. 2015. An ecological engineer maintains consistent spatial patterning, with implications for community-wide effects. Ecosphere 6:151.

Dunkerley, D. L. 2010. Ecogeomorphology in the Australian drylands and the role of biota in mediating the effects of climate change on landscape processes and evolution. Geological Society, London, Special Publications 346:87–120.

Dunkerley, D. L., and K. J. Brown. 2002. Oblique vegetation banding in the Australian arid zone: implications for theories of pattern evolution and maintenance. Journal of Arid Environments 51:163–181.

Getzin, S., R. Nuske, and K. Wiegand. 2014. Using unmanned aerial vehicles (UAV) to quantify spatial gap patterns in forests. Remote Sensing 6:6988–7004.

Getzin, S., K. Wiegand, and I. Schöning. 2012. Assessing biodiversity in forests using very high-resolution images and unmanned aerial vehicles. Methods in Ecology and Evolution 3:397–404.

Getzin, S., K. Wiegand, T. Wiegand, H. Yizhaq, J. von Hardenberg, and E. Meron. 2015a. Adopting a spatially explicit perspective to study the mysterious fairy circles of Namibia. Ecography 38:1–11.

Getzin, S., K. Wiegand, T. Wiegand, H. Yizhaq, J. von Hardenberg, and E. Meron. 2015b. Clarifying misunderstandings regarding vegetation self-organization and spatial patterns of fairy circles in Namibia: a response to recent termite hypotheses. Ecological Entomology 40:669–675.

Getzin, S., et al. 2016a. Discovery of fairy circles in Australia supports self-organization theory. Proceedings of the National Academy of Sciences 113:3551–3556.

Getzin, S., et al. 2016b. Reply to Walsh et al.: Hexagonal patterns of Australian fairy circles develop without correlation to termitaria. Proceedings of the National Academy of Sciences 113:E5368–E5369.

Goudie, A. S., and H. A. Viles. 2015. Landscapes and landforms of Namibia. Springer, Dordrecht, The Netherlands.

Grohmann, C., J. Oldeland, D. Stoyan, and K. E. Linsenmair. 2010. Multi-scale pattern analysis of a mound-building termite species. Insectes Sociaux 57:477–486.

Holt, J. A., and J. F. Easey. 1985. Polycalic colonies of some mound building termites (Isoptera: Termitidae) in northeastern Australia. Insectes Sociaux 32:61–69.

Illian, J., A. Penttinen, H. Stoyan, and D. Stoyan. 2008. Statistical analysis and modelling of spatial point patterns. Wiley and Sons, Chichester, UK.

Isbell, R. F. 2002. The Australian soil classification. Rev. Edition. CSIRO Publications, Collingwood, Victoria, Australia.

Juergens, N. 2013. The biological underpinnings of Namib Desert fairy circles. Science 339:1618–1621.

Lefever, R., and O. Lejeune. 1997. On the origin of tiger bush. Bulletin of Mathematical Biology 59: 263–294.

Ludwig, J. A., B. P. Wilcox, D. D. Breshears, D. J. Tongway, and A. C. Imeson. 2005. Vegetation patches and runoff-erosion as interacting ecohydrological processes in semiarid landscapes. Ecology 86:288–297.

Mabbutt, J. A., and P. Fanning. 1987. Vegetation banding in arid Western Australia. Journal of Arid Environments 12:41–59.

McGlynn, T. P. 2012. The ecology of nest movement in social insects. Annual Review of Entomology 57:291–308.

McIntire, E. J. B., and A. Fajardo. 2009. Beyond description: the active and effective way to infer processes from spatial patterns. Ecology 90:46–56.

Meron, E. 2012. Pattern-formation approach to modelling spatially extended ecosystems. Ecological Modelling 234:70–82.

Meron, E. 2018. From patterns to function in living systems: dryland ecosystems as a case study. Annual Review of Condensed Matter Physics 9:79–103.

Meyer, J. J. M., F. Senejoux, H. M. Heyman, N. L. Meyer, and M. A. Meyer. 2015. The occurrence of triterpenoids from *Euphorbia gummifera* inside the fairy circles of Garub in the southern Namibian prodesert. South African Journal of Botany 98:10–15.

Morton, S. R., et al. 2011. A fresh framework for the ecology of arid Australia. Journal of Arid Environments 75:313–329.

Naude, Y., M. W. van Rooyen, and E. R. Rohwer. 2011. Evidence for a geochemical origin of the mysterious circles in the Pro-Namib desert. Journal of Arid Environments 75:446–456.

Nicolai, N., R. A. Feagin, and F. E. Smeins. 2010. Spatial patterns of grass seedling recruitment imply predation and facilitation by harvester ants. Environmental Entomology 39:127–133.

Noble, J., P. Diggle, and W. Whitford. 1989. The spatial distributions of termite pavements and hummock feeding sites in a semi-arid woodland in eastern Australia. Acta Oecologica Oecologia Generalis 10:355–376.

Pepper, M., P. Doughty, and J. Keogh. 2013. Geodiversity and endemism in the iconic Australian Pilbara region: a review of landscape evolution and biotic response in an ancient refugium. Journal of Biogeography 40:1225–1239.

Perry, G. L. W., B. P. Miller, and N. J. Enright. 2006. A comparison of methods for the statistical analysis of spatial point patterns in plant ecology. Plant Ecology 187:59–82.

Picker, M. D., V. Ross-Gillespie, K. Vlieghe, and E. Moll. 2012. Ants and the enigmatic Namibian fairy circles – Cause and effect? Ecological Entomology 37:33–42.

Ramond, J. B., A. Pienaar, A. Armstrong, M. Seely, and D. A. Cowan. 2014. Niche-partitioning of edaphic microbial communities in the Namib Desert gravel plain Fairy Circles. PLoS ONE 9:e109539.

Ravi, S., L. Wang, K. F. Kaseke, I. V. Buynevich, and E. Marais. 2017. Ecohydrological interactions within "fairy circles" in the Namib Desert: revisiting the self-organization hypothesis. Journal of Geophysical Research: Biogeosciences 122:405–414.

Rice, B., and M. Westoby. 2009. Regeneration after fire in *Triodia* R. Br. Australian Journal of Ecology 24:563–572.

Rietkerk, M., M. C. Boerlijst, F. Van Langevelde, R. Hillerislambers, J. Van De Koppel, L. Kumar, H. H. T.

Prins, and A. M. De Roos. 2002. Self-organization of vegetation in arid ecosystems. American Naturalist 160:524–530.

Saco, P. M., G. R. Willgoose, and G. R. Hancock. 2007. Eco-geomorphology of banded vegetation patterns in arid and semi-arid regions. Hydrology and Earth System Sciences Discussions 11:1717–1730.

Sahagian, D. 2017. The magic of fairy circles: Built or created? Journal of Geophysical Research: Biogeosciences 122:1294–1295.

Schooley, R. L., and J. A. Wiens. 2003. Spatial patterns, density dependence, and demography in the harvester ant, *Pogonomyrmex rugosus* in semi-arid grasslands. Journal of Arid Environments 53:183–196.

Schurr, F. M., O. Bossdorf, S. J. Milton, and J. Schumacher. 2004. Spatial pattern formation in semi-arid shrubland: a priori predicted versus observed pattern characteristics. Plant Ecology 173:271–282.

Sheffer, E., H. Yizhaq, E. Gilad, M. Shachak, and E. Meron. 2007. Why do plants in resource-deprived environments form rings? Ecological Complexity 4:192–200.

Spain, A. V., D. F. Sinclair, and P. J. Diggle. 1986. Spatial distributions of the mounds of harvester and forager termites (Isoptera: Termitidae) at four locations in tropical North-Eastern Australia. Acta Oecologica Oecologia Generalis 7:335–352.

Tarnita, C. E., J. A. Bonachela, E. Sheffer, J. A. Guyton, T. C. Coverdale, R. A. Long, and R. M. Pringle. 2017. A theoretical foundation for multi-scale regular vegetation patterns. Nature 541:398–401.

Tongway, D. J., and J. A. Ludwig. 1990. Vegetation and soil patterning in semi-arid mulga lands of Eastern Australia. Australian Journal of Ecology 15:23–34.

Tschinkel, W. R. 2010. The foraging tunnel system of the Namibian desert termite, *Baucaliotermes hainesi*. Journal of Insect Science 10:1–17.

Tschinkel, W. R. 2012. The life cycle and life span of Namibian fairy circles. PLoS ONE 7:e38056.

Tschinkel, W. R. 2015a. Biomantling and bioturbation by colonies of the Florida harvester ant, *Pogonomyrmex badius*. PLoS One 10:e0120407.

Tschinkel, W. R. 2015b. Experiments testing the causes of Namibian fairy circles. PLoS ONE 10:e0140099.

van Rooyen, M. W., G. K. Theron, N. van Rooyen, W. J. Jankowitz, and W. S. Matthews. 2004. Mysterious circles in the Namib Desert: review of hypotheses on their origin. Journal of Arid Environments 57:467–485.

Walsh, F. J., A. D. Sparrow, P. Kendrick, and J. Schofield. 2016. Fairy circles or ghosts of termitaria? Pavement termites as alternative causes of circular

patterns in vegetation of desert Australia. Proceedings of the National Academy of Sciences 113: E5365–E5367.

Watson, J. A. L., C. Lendon, and B. S. Low. 1973. Termites in mulga lands. Tropical Grasslands 7:121–126.

Wiegand, T., F. He, and S. P. Hubbell. 2013. A systematic comparison of summary characteristics for quantifying point patterns in ecology. Ecography 36:92–103.

Wiegand, T., and K. A. Moloney. 2014. Handbook of spatial point pattern analysis. Chapman and Hall, Boca Raton, Florida, USA.

Wiernasz, D. C., and B. J. Cole. 1995. Spatial distribution of *Pogonomyrmex occidentalis*: recruitment, mortality and overdispersion. Journal of Animal Ecology 64:519–527.

Zelnik, Y. R., E. Meron, and G. Bel. 2015. Gradual regime shifts in fairy circles. Proceedings of the National Academy of Sciences 112:12327–12331.

Supporting Information

Additional Supporting Information may be found online at: http://onlinelibrary.wiley.com/doi/10.1002/ecs2.2620/full

A multi-scale study of Australian fairy circles using soil

excavations and drone-based image analysis

Stephan Getzin, Hezi Yizhaq, Miriam Muñoz-Rojas, Kerstin Wiegand, and Todd E. Erickson
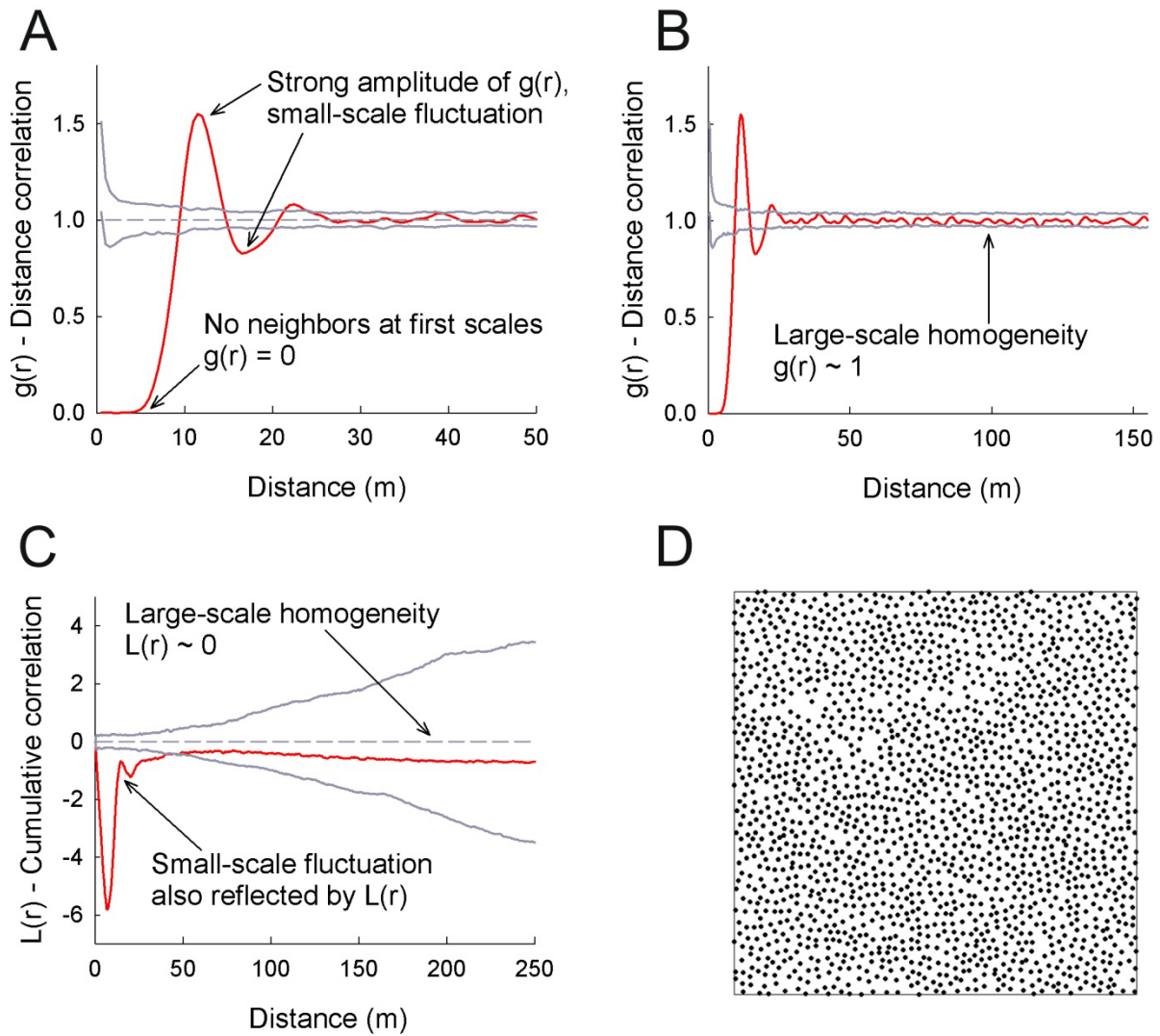
Appendix S1

Fig. S1. Spatial pattern analysis of FCs using the pair-correlation function $g(r)$ and the cumulative *L*-function. The pair-correlation function (red line) detects no neighbors (zero values) for very small radii and fluctuates thereafter strongly around the random null model (grey simulation envelopes) which indicates a grid-like hexagonal pattern (A). The first pronounced peak with a strong amplitude at around 10 m distance indicates the mean-nearest neighbor distance of the FCs. At large scales, $g(r)$ approaches values of 1, indicating large-scale homogeneity (B). Similarly, if the cumulative *L*-function, after the first small-scale deviations from CSR (Complete Spatial Randomness), moves consistently into the envelopes of the simulated CSR null model, this indicates a pattern that is large-scale homogeneous (C). The analyses are demonstrated for the 500 m × 500 m plot FC-C2 (D).

Fig. S2. Variable amounts of vegetation inside FCs. A large FC in the plot FC-L2 with a *Triodia* plant in the center and a small termite mound at the upper right gap edge (A). Growth of the grass in the center was not affected by any hard pavement layer, despite the vicinity of the mound (B). Fairy circles often show variable numbers of individual *Triodia* or *Aristida* grass plants growing in the large gaps (C-H). The substrate does not show hard pavement termitaria under the soil surface, with plant rooting and growth not inhibited locally (I). The abiotic mechanism which leads to bare-soil gaps as shown in (H) is likely the same that hampers plant establishment and long-term survival in the large bare-soil areas such as in the plot FC-B (J).
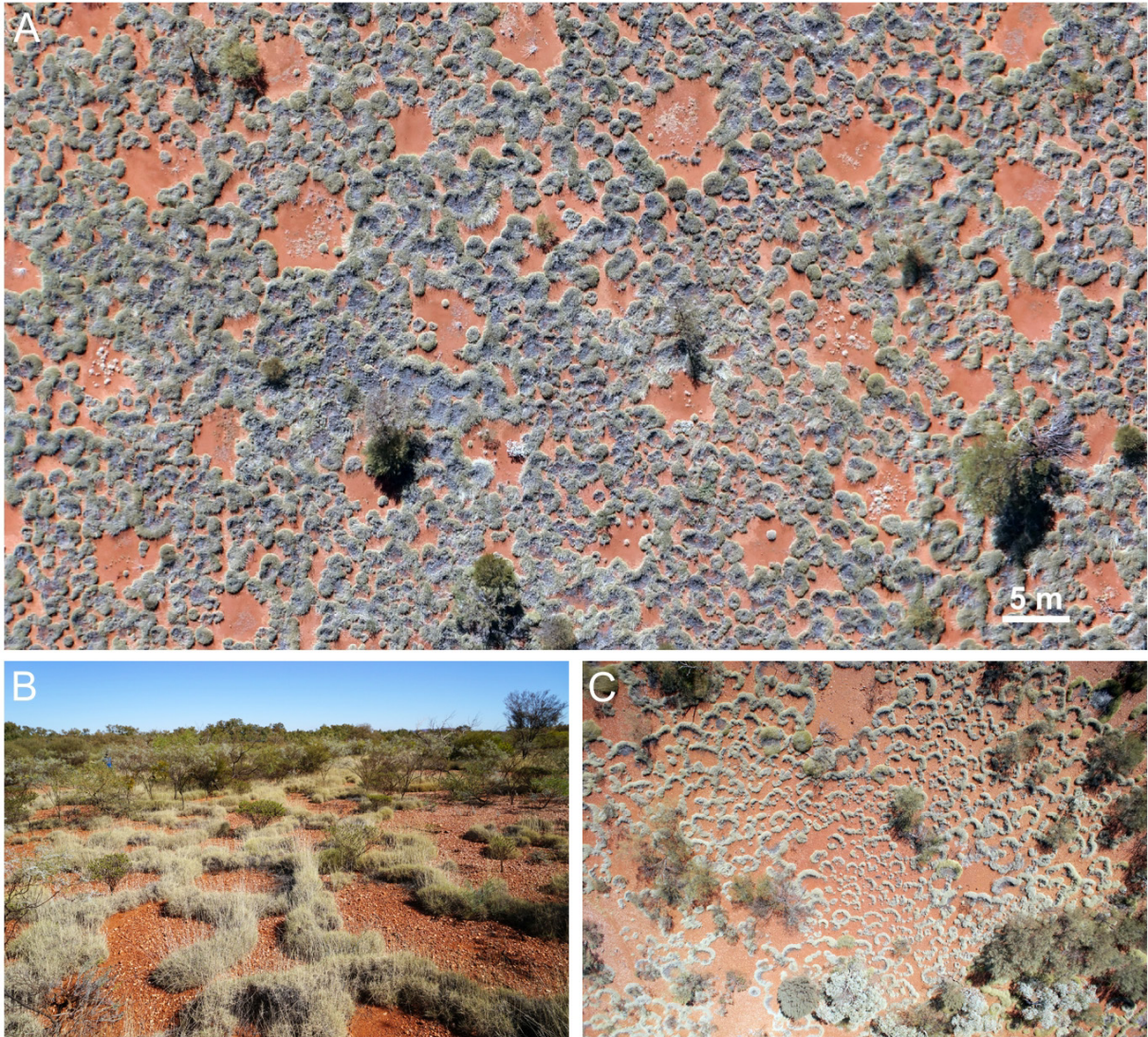
Fig. S3. Drone image showing parts of the plot FC-L2 (A). Fairy circles have variable occupations of vital or senescent grasses, indicating that gap formation is subject to a dynamic change. Note the small irregularly shaped gaps appearing at various places in the matrix vegetation. *Triodia* plants build gap-labyrinth transitions at a sloping terrain near the FC-L2 plot, close to the Ophthalmia Dam (B,C).
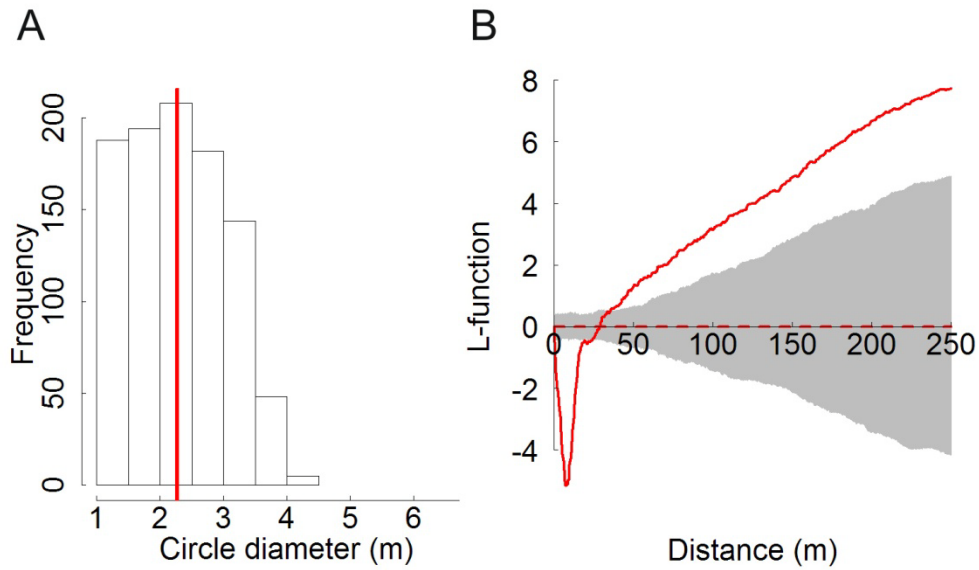
Fig. S4. Histogram of the diameter distribution of gaps created by harvester termites in the drone-mapped plot HT-1, using a diameter threshold of 1 m (A). The red vertical line shows the median diameter which declined to 2.3 m (from 2.7 m, using the 2 m threshold). The spatial distribution pattern of gaps created by harvester termites in HT-1, using the same 1 m size threshold (B). The pattern is heterogeneously distributed at the landscape scale if the red line of the *L*-function is at larger distances > 50 m above the upper grey simulation envelopes of the homogeneous Poison null model, CSR. The above example demonstrates that inclusion of the smallest diameters ≥ 1 m leads also to large-scale heterogeneous termite gaps. This analysis could not be shown for the plot HT-2 since the gaps of this plot were not clearly detectable below a threshold of 2 m diameter.